ISSN 1001-0742
CN 11-2629/X

JOURNAL OF ENVIRONMENTAL SCIENCES

May 1, 2015 Volume 31
www.jesc.ac.cn

Real-world diesel vehicle emission factors for China

ELSEVIER
Science Press

Sponsored by
Research Center for Eco-Environmental Sciences
Chinese Academy of Sciences

Journal of Environmental Sciences Volume 31 2015

www.jesc.ac.cn

Highlight articles

Review articles

Regular articles

CONTENTS

Available online at www.sciencedirect.com

ScienceDirect

www.journals.elsevier.com/journal-of-environmental-sciences

JOURNAL OF ENVIRONMENTAL SCIENCES
www.jesc.ac.cn

Effect of water vapor on NH_3–NO/NO_2 SCR performance of fresh and aged MnOx–NbOx–CeO_2 catalysts

Lei Chen[1], *Zhichun Si*[2], *Xiaodong Wu*[1], *Duan Weng*[1,*], *Zhenwei Wu*[1]

1. *State Key Lab of New Ceramics and Fine Processing, School of Materials Science and Engineering, Tsinghua University, Beijing 100084, China*
2. *Graduate School at Shenzhen, Tsinghua University, Shenzhen 518055, China*

ARTICLE INFO

Article history:
Received 17 May 2014
Revised 10 July 2014
Accepted 17 July 2014
Available online 20 February 2015

Keywords:
Water effect
MnOx–NbOx–CeO_2 catalysts
Acid sites
Fast SCR reaction
NO/NO_2 ratio

ABSTRACT

A MnOx–NbOx–CeO_2 catalyst for low temperature selective catalytic reduction (SCR) of NOx with NH_3 was prepared by a sol–gel method, and characterized by NH_3–NO/NO_2 SCR catalytic activity, NO/NH_3 oxidation activity, NOx/NH_3 TPD, XRD, BET, H_2-TPR and *in-situ* Diffuse Reflectance Infrared Fourier Transform Spectroscopy (DRIFTS). The results indicate that the MnOx–NbOx–CeO_2 catalyst shows excellent low temperature NH_3-SCR activity in the temperature range of 150–300°C. Water vapor inhibits the low temperature activity of the catalyst in standard SCR due to the inhibition of NOx adsorption. As the NO_2 content increases in the feed, water vapor does not affect the activity in NO_2 SCR. Meanwhile, water vapor significantly enhances the N_2 selectivity of the fresh and the aged catalysts due to its inhibition of the decomposition of NH_4NO_3 into N_2O.

Introduction

The concept of the reduction of NO and NO_2 on FeOx–TiO_2 mixed oxide catalysts was first introduced by Kato in the year 1981 (Kato et al., 1981), and has attracted much attention since then. Unlike the standard NH_3-SCR reaction (Eq. (1)), "fast SCR" (Eq. (2)) is the reaction between NH_3 and a mixture of equimolar NO and NO_2, with much faster reaction rate (Koebel et al., 2002; Nova et al., 2006; Grossale et al., 2008; Iwasaki and Shinjoh, 2010; Ruggeri et al., 2012). When NO_2 is predominant, it will react with NH_3 directly *via* alternative NO_2 SCR (Eqs. (3) or (4)). The reaction rate of NO_2 SCR is much slower than that of the fast SCR reaction above 200°C and involves N_2O and NH_4NO_3 formations. Tronconi et al. (2007) pointed out the key catalytic role of vanadium redox behavior, which can explain the higher catalytic activity of fast SCR than standard SCR. Grossale et al. (2008) studied the stoichiometry, selectivity and kinetics of fast SCR on Fe-ZSM5 catalysts, and further confirmed that the reaction between NO and nitrates was the rate-controlling step, which was inhibited by ammonia; the study also explained that N_2O formed by the decomposition of the NH_4NO_3 intermediate when NO_2 predominated. Iwasaki and Shinjoh (2010) studied different NO/NO_2 ratios and N_2O formation over Fe/zeolite catalysts, and their results also indicated that N_2O formation reached a maximum at 250°C due to the decomposition of the NH_4NO_3 intermediate in NO_2 SCR.

$$4NH_3 + 4NO + O_2 \rightarrow 4N_2 + 6H_2O \quad (1)$$

$$2NH_3 + NO + NO_2 \rightarrow 2N_2 + 3H_2O \quad (2)$$

$$2NH_3 + 2NO_2 \rightarrow N_2 + N_2O + 3H_2O \quad (3)$$

* *Corresponding author*. E-mail: duanweng@mail.tsinghua.edu.cn (Duan Weng).

http://dx.doi.org/10.1016/j.jes.2014.07.037

$$4NH_3 + 3NO_2 \rightarrow 7/2N_2 + 6H_2O \quad (4)$$

Mn-containing catalysts, especially MnOx–CeO_2 catalysts, have attracted lots of attention because of their excellent low temperature SCR activity (Li et al., 2011a, b). However, low N_2 selectivity and poor resistance to humidity are major problems with Mn-based catalysts. Yang's group (Qi and Yang, 2003a, b, 2004; Qi et al., 2004) reported that MnOx–CeO_2 catalysts had an excellent low temperature (80–140°C) activity, which was zero order with respect to NH_3 and first order with respect to NO. Casapu et al. (2009, 2010) studied the effects of different dopants including niobium, iron, tungsten and zirconium oxide on the low-temperature activity of MnOx–CeO_2 catalysts for the NH_3-SCR of NOx on coated cordierite monoliths; the results indicated that Nb_2O_5 significantly enhanced the catalytic activity (180–330°C) and N_2 selectivity of the MnOx–CeO_2 catalyst. Many other transition metals used as dopants (SnO_2, FeOx or WO_3) were investigated to improve the low temperature performance of MnOx–CeO_2 catalysts (Chang et al., 2013; Shen et al., 2010; Zhang et al., 2011) The supports of MnOx–CeO_2 catalysts, such as TiO_2, Al_2O_3, ZrO_2, active carbon, and pillar clay, have also been extensively studied in recent years (Jin et al., 2010; Shen et al., 2011, 2013, 2014; Xu et al., 2012).

Niobium modification was revealed to be an effective method to improve the acidity and niobium-containing catalysts also showed potential applications in selective catalytic reduction of NOx with ammonium or hydrocarbons (Casapu et al., 2011; Du et al., 2012; Ma et al., 2012). The Nb–OH bond is responsible for Brønsted acid sites and the Nb═O bond for Lewis acid sites (Qu et al., 2014), both of which are important in the NH_3-SCR reaction. However, the effect of water vapor on the NH_3–NO/NO_2 SCR reaction still needs to be investigated in depth, especially SCR reactions on niobium-modified MnOx–CeO_2. In this study, the NH_3–NO/NO_2 SCR performance of MnNbCe mixed oxide catalysts was investigated and the effects of water on different NO/NO_2 ratios over fresh and hydrothermally aged MnNbCe mixed oxide catalysts were studied.

1. Experimental

1.1. Catalyst preparation

The MnNbCe mixed oxide catalyst was prepared by a sol–gel method. Manganese acetate (Beijing Chem. Plant), niobium oxalate (Aladdin), cerium nitrate hexahydrate (Aladdin), citric acid (Aladdin), nitric acid (Beijing Chem. Plant) were all analytical reagents.

The nitric acid and citric acid were dissolved in deionized water first. The niobium oxalate, manganese acetate and cerium nitrate hexahydrate were then added into the solution, respectively. The molar ratio of Nb, Mn and Ce used was 1:1:3 and the molar ratio of metal components (the total moles of Nb, Mn and Ce) to citric acid to nitric acid was 1:1.5:1.5. The solutions were stirred and heated for 5 hr to form a gel, then the gels were dried at 110°C overnight and calcined in a muffle furnace at 500°C for 5 hr to obtain the fresh catalyst. The aged MnNbCe catalyst was obtained by deactivating the catalyst at 800°C in 10% H_2O for 8 hr. Finally, the samples were crushed and sieved to 50–80 mesh for catalytic activity measurements. The fresh and aged MnNbCe catalysts are denoted as MnNbCe-F and MnNbCe-A, respectively.

1.2. Activity measurements

The catalytic activity measurement for the reduction of NO_x by ammonia (NH_3–NO/NO_2 SCR) with excess oxygen was carried out in a fixed bed reactor made of a quartz glass tube. 0.2 g catalysts with 50–80 mesh size were diluted to 1 mL by silica. The reaction gas mixture simulating diesel engine exhaust gases consisted of 500 ppm NOx (including NO and NO_2), 500 ppm NH_3, and 5% O_2 and N_2 in balance. For the fast SCR reaction the ratio of NO:NO_2 is 1:1. For the NO SCR or NO_2 SCR reactions, only NO or NO_2 was introduced into the feed gas. The NOx conversion was measured when the reactant gas was stably fed for 30 min at various temperatures from 100 to 300°C. The total flow of the gas mixture was 1 L/min at a gas hourly space velocity (GHSV) of 30,000 hr^{-1}. The concentrations of nitrogen oxides and ammonia were measured at 120°C by a Thermo Nicolet 380 FT-IR spectrometer equipped with a 2 m path-length sample cell (250 mL volume). The gas path from the reactor to FT-IR spectrometer was maintained at a constant temperature of 120°C to avoid NH_4NO_2/NH_4NO_3 deposition. The NOx conversion and N_2 selectivity were calculated according to Eqs. (5) and (6).

$$NO_x\ \text{conversion}(\%) = 1 - \frac{NO_{out} + NO_{2out}}{NO_{in}} \times 100 \quad (5)$$

$$N_2\ \text{selectivity}(\%) = 1 - \frac{NH_{3out} + NO_{out} + NO_{2out}}{NH_{3in} - NH_{3out} + NO_{in} - NO_{out}} \times 100 \quad (6)$$

NH_3 oxidation and NO oxidation tests were carried out using a method similar to that for NH_3-SCR activity with 500 ppm NH_3 (500 ppm NO for NO oxidation) and 5% O_2 in N_2 balance. The NH_3 or NO conversion was measured after 30 min of steady state reaction at various temperatures from 100 to 400°C.

NH_3-TPD and NOx-TPD tests were carried out using a similar method to that used for NH_3-SCR activity. 0.2 g catalyst with 0.8 mL silica sand was first pretreated in 8% O_2, N_2 balance, 500°C for 30 min. Then the catalyst was cooled down to 100°C and saturated in 500 ppm NH_3 for NH_3-TPD or 500 ppm NO + 5% O_2 for NO-TPD or 500 ppm NO_2 for NO_2-TPD, 10% H_2O if introduced, N_2 balance for 30 min isothermal desorption in N_2 at room temperature until no NOx (NH_3) was detected, then temperature programmed desorption carried out in N_2 at 10°C/min to 500°C.

1.3. Catalyst characterization

The powder X-ray diffraction (XRD) experiments were performed on a German Bruker D8 ADVANCE diffractometer employing Cu Kα radiation (λ = 0.15418 nm). The X-ray tube was operated at 40 kV and 40 mA. The X-ray powder patterns were recorded at 6°/min in the range $10° < 2\theta < 80°$. The identification of the phases was made with the help of JCPDS (Joint Committee on Powder Diffraction Standards) cards. The

mean crystallite sizes were calculated by the Scherrer formula.

The specific surface areas and pore volumes of the catalyst were measured by nitrogen physisorption at liquid nitrogen temperature using a surface area and pore size analyzer (JW-BK122F, Beijing JWGB Sci. & Tech.). The catalysts were degassed at 220°C for 2 hr prior to the measurements. The pore volumes for the samples were calculated by the BJH (Barrett–Joyner–Halenda) method.

A Thermo Nicolet 6700 Fourier Transform Infrared (FT-IR) spectrometer was equipped with a high-temperature environmental cell fitted with a KBr window. *In-situ* FT-IR spectra of adsorbed species were recorded in the range of 4000–650 cm^{-1}. Prior to the adsorption, the sample was placed in a crucible located in a high-temperature cell and heated up to 500°C in a 20% (V/V) O_2/N_2 flow mixture with a total flow of 100 mL for 30 min to remove traces of organic residues. After that, the sample was cooled down to room temperature and was flushed by 100 mL/min N_2 for 30 min to remove the physisorbed molecules for background collection. For the NH_3 adsorption, a gas mixture containing 1000 ppm NH_3 in N_2 with a total flow rate of 100 mL/min was passed through the sample for 60 min. After purging the weakly adsorbed or gaseous NH_3 molecules by N_2 flow for 30 min, the FT-IR spectra of adsorbed species on catalysts were collected simultaneously.

H_2-TPR experiments were conducted on a Micromeritics Autochem II 2920 chemisorption analyzer using 50 mg of the MnNbCe samples. The samples were preheated at 500°C for 30 min in He flow. The H_2-TPR was carried out from 50 to 1000°C at a heating rate of 10°C/min with 10% H_2/Ar gases. The H_2 consumption was recorded continuously.

2. Results and discussion

2.1. XRD and BET

The XRD patterns of MnNbCe catalysts are shown in Fig. 1. The main phase of the MnNbCe catalysts is the cubic fluorite structure of ceria. For the fresh MnNbCe catalyst, no distinct peak detected can be assigned to Nb_2O_5 or MnOx species, indicating that MnO_x and NbOx species are highly dispersed on cubic fluorite structure ceria. After hydrothermal aging, sharp peaks assigned to cubic ceria and Mn_2O_3 appear due to the strong sintering and crystallization of these metal oxides. It is clear that hydrothermal aging leads to solid-state reaction between manganese species and niobium oxides with the formation of $MnNb_2O_6$, consistent with results in the literature (Casapu et al., 2009). Structural parameters of the MnNbCe catalysts are shown in Table 1. After hydrothermal aging, the BET surface area decreased from 107 to 67 m^2/g. The total pore volume of aged catalysts showed a sharp decrease and the average pore diameter increased, which may originate from the $MnNb_2O_6$ formation and further crystallization during the hydrothermal aging.

2.2. Redox properties

The NH_3 adsorption and H_2-TPR profiles of fresh and aged MnNbCe catalysts are shown in Fig. 2. For NH_3 adsorption on

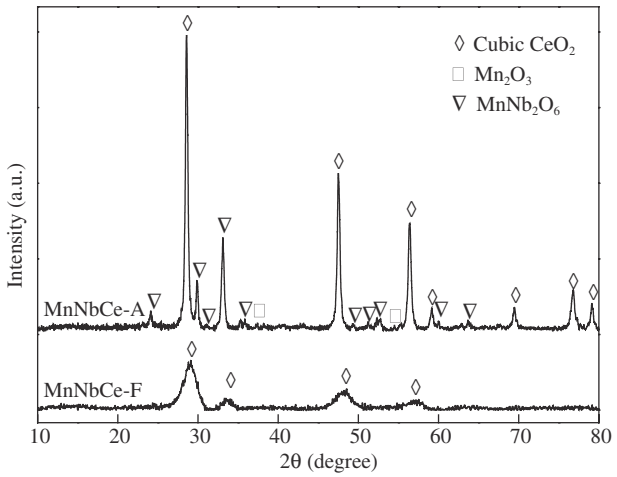

Fig. 1 – XRD patterns of the MnNbCe catalysts.

the fresh MnNbCe catalyst, the bands at 1670 and 1430 cm^{-1} can be assigned to the σ_s NH_4^+ and σ_{as} NH_4^+ vibrations on Brønsted acid sites (Zawadzki and Wiśniewski, 2003). The bands at 1600 and 1137–1196 cm^{-1} can be attributed to the σ_{as} NH_3 and σ_s NH_3 vibrations on Lewis acid sites (Ramis et al., 1995; Larrubia et al., 2000, 2001; Chen et al., 2010). In the N–H region, bands at 3369 and 3247 cm^{-1} were detected. Negative bands around 3800 cm^{-1} attributed to O–H were detected (Sun et al., 2009). As temperature increased, all of the NH_3 adsorption bands decreased. The bands at 1137–1196 cm^{-1} shifted to higher wavenumbers as temperature increased. Both the Brønsted and Lewis acid site bands of NH_3 decreased sharply after hydrothermal aging, especially for the Lewis acid sites. The bands at 1137–1196 cm^{-1} assigned to NH_3 on Lewis acid sites shifted to higher wavenumbers at 1206 cm^{-1}.

The H_2-TPR profiles of the MnNbCe catalysts are shown in Fig. 2b. Bands at 339, 415 and 587°C were detected for fresh catalyst. The peaks at 339 and 415°C correspond to a gradual reduction of MnO_2 or $Mn_2O_3 \rightarrow Mn_3O_4$ and $Mn_3O_4 \rightarrow MnO$ (Carnö et al., 1997; Tang et al., 2006; Li et al., 2011a, b). The peak at 587°C is associated with the reduction of Ce^{4+} to Ce^{3+} (Liu et al., 2014). For aged catalyst, only two peaks at 393 and 747°C were seen, corresponding to the reduction of $Mn_3O_4 \rightarrow MnO$ and the reduction of bulk CeO_2, respectively (Ettireddy et al., 2007). The results indicate that strong sintering and crystallization of CeO_2 and MnOx species inhibited the redox abilities of the MnNbCe catalyst.

2.3. NH_3/NO oxidation

The NO oxidation to NO_2 on fresh and aged MnNbCe catalyst is shown in Fig. 3a. The results indicate that the fresh catalyst

Table 1 – Structural parameters of the MnNbCe catalysts.

Sample	BET surface area (m^2/g)	Total pore volume (cm^3/g)	Average pore diameter (nm)
MnNbCe-F	107	0.251	6.0
MnNbCe-A	67	0.048	8.5

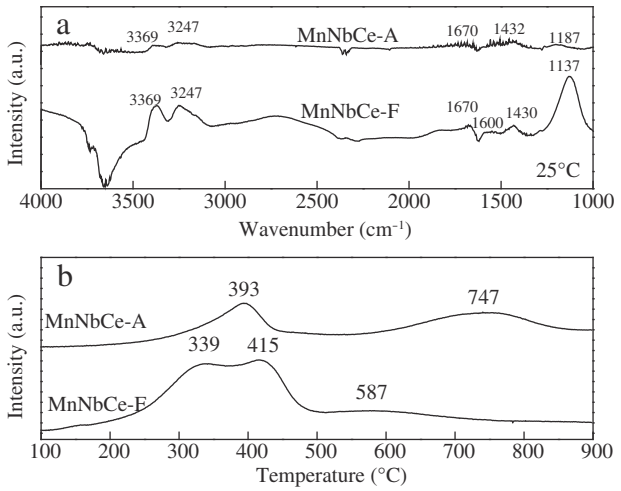

Fig. 2 – NH_3 adsorption at 25°C (a) and H_2-TPR profiles (b) of the MnNbCe catalysts.

showed much better NO oxidation activity in the whole temperature range. The NO conversion on the fresh MnNbCe catalyst increased with increasing temperature and the profile shows a peak of 56% NO conversion at 350°C. For the aged MnNbCe catalyst, the NO oxidation activity kept increasing with elevated temperature, with a peak value around 21% at 400°C.

The NH_3 oxidation activity and N_2O formation of MnNbCe catalysts are shown in Fig. 3b. The NH_3 oxidation activity of fresh catalyst is much higher than that of aged catalyst. The onset temperature of NH_3 oxidation of fresh catalyst is around 160°C and reaches 100% at 300°C. For aged catalyst, the NH_3 oxidation started above 200°C and increased with increasing temperature, reaching a peak of 96% NH_3 conversion at 400°C. A

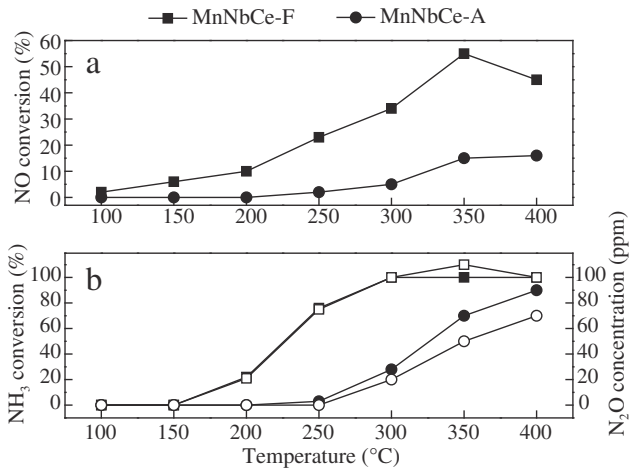

Fig. 3 – NH_3/NO oxidation activities of MnNbCe catalysts as a function of temperature. Reaction conditions: [NH_3/NO] = 500 ppm, [O_2] = 5%, N_2 balances, GHSV 30,000 h^{-1}. Filled symbol: conversion, open symbol: N_2O concentration.

similar trend was found for N_2O formation, with the NH_3 oxidation and N_2O formation being more pronounced over fresh catalyst.

2.4. NH_3/NOx TPD

In order to confirm the effect of water on the NH_3 and NOx adsorption, NH_3/NOx-TPD experiments were carried out and the results of NH_3-TPD are shown in Fig. 4. The amount of the desorbed species over fresh MnNbCe catalysts is shown in Table 2. Results indicate that NH_3 desorption on MnNbCe catalysts shows a peak of 80 ppm at around 180°C. The amount of NH_3 species desorbed is similar in the absence (0.35 mmol) and presence (0.34 mmol) of water vapor. The results indicate that water vapor addition has only a slight effect on NH_3 adsorption, leading to a shift in the NH_3 desorption peak to lower temperature.

The effect of water vapor on NOx-TPD was investigated and the results are shown in Fig. 5. The results of NO + O_2 TPD indicate a peak of 60 ppm NO_2 desorbed at 210°C, and the amount of desorbed NO_2 was much more than that of desorbed NO. When water vapor was added in the feed, the amount desorbed NO_2 species was halved compared with that without water vapor addition. The peak of NO_2 desorption shifted from 210 to 250°C, which means that water addition strongly inhibits the adsorption of NO_2 on the catalyst surface. At the same time, the NO adsorption was increased after water addition. The effect of water vapor on NO_2 adsorption is shown in Fig. 5b. The results show that a peak of 140 ppm NO_2 was desorbed at 210°C. Compared with NO + O_2 adsorption, NO_2 is more easily adsorbed on the catalyst. The amount of NO_2 adsorbed in the NO_2 feed was much larger than that in the NO + O_2 feed. Meanwhile, water addition barely affected the amount of NO_2 adsorption.

2.5. Catalytic activity of NH_3–NO–NO_2 SCR

The NH_3–NO/NO_2 SCR activities of fresh and aged MnNbCe catalysts are shown in Fig. 6. The fresh MnNbCe catalyst showed excellent low temperature activity in the NH_3–NO/NO_2 SCR reaction and the activities of the fresh MnNbCe catalyst rank as fast SCR > standard SCR > NO_2 SCR. For fast SCR, the fresh catalyst showed high catalytic activity (>80%) in the low temperature range of 150–300°C, while the working temperature narrowed to 180–300°C for NO_2 SCR. The hydrothermal aging led to a severe decrease in the activity of NO SCR, while the affect was weakened as the ratio of NO_2 in the feed increased. For standard SCR, the catalytic activity of catalysts decreased in the whole temperature range after hydrothermal aging. For fast and NO_2 SCR, the loss in catalytic activity was weakened after hydrothermal aging, mainly in the low temperature range of 100–200°C.

The water vapor addition also showed distinct effects on the NH_3–NO/NO_2 SCR activity of fresh catalyst at various NO_2 feed levels. Generally, the effect of water vapor on the catalytic activity of fresh MnNbCe catalyst for standard SCR was more significant. The addition of water vapor decreased the activity of catalyst for standard SCR in the whole temperature range, especially at temperatures below 200°C. For the fast SCR reaction, the addition of water vapor only

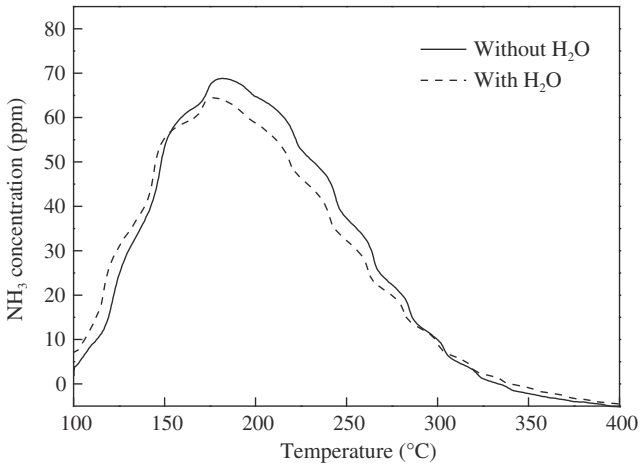

Fig. 4 – NH_3 TPD over fresh MnNbCe catalyst.

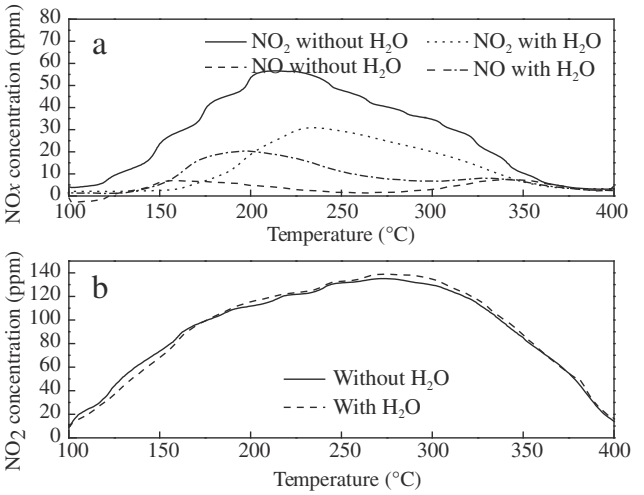

Fig. 5 – NO + O_2 TPD (a) and NO_2 TPD (b) over fresh MnNbCe catalyst.

decreased the activity at temperatures below 200°C for fresh MnNbCe catalyst. The addition of water vapor slightly decreased the catalytic activity of NO_2 SCR at much lower temperatures below 200°C, after which the catalytic activity was even higher than that in the absence of water vapor.

Hydrothermal aging led to strong sintering and crystallization of Mn species and formation of $MnNb_2O_6$, as well as a decrease in the redox ability and number of acid sites. The catalytic activity loss due to hydrothermal aging was much less for fast SCR and NO_2 SCR compared with the standard SCR, especially at high temperature. The effect of water vapor addition over the aged MnNbCe catalyst was weak and mainly seen in NO SCR at temperatures above 150°C, while the effect on fast and NO_2 SCR was negligible.

Shi et al. (2013) reported that aged Fe-ZSM-5 showed a significant decrease in the low-temperature activity and a slight increase in the high-temperature activity. Sung's group (Kim et al., 2010) reported that NO_2 was superior to O_2 to re-oxidize the active V species at low temperature. Results indicated that when NO_2 was added in the feed gas, the loss in catalytic activity decreased, because NO_2 is much more easily adsorbed on the surface of the catalyst and re-oxidizes the active site of the catalyst. This is also the reason that water had little influence on the catalytic activity when NO_2 was introduced.

2.6. Catalytic activity of NH_3–NO–NO_2 SCR

The production of N_2O is the major disadvantage of the addition of NO_2 into the feed to enhance the NOx conversion over MnNbCe catalysts. The N_2O formation for NH_3–NO/NO_2 SCR over fresh and aged MnNbCe catalysts is shown in Fig. 7. The results illustrate that N_2O formation increases as the temperature increases and reaches a maximum of 98 ppm at 300°C for fresh catalyst in the standard SCR reaction. For aged catalyst, the catalytic activity shows a sharp decrease after aging, and the amount of N_2O formation over fresh and aged catalyst is similar. For the fast SCR reaction, more N_2O was formed and reached a maximum of 98 ppm at 300°C. Similar behavior was found in fast SCR and the NO_2 SCR reaction, with increased N_2O formation. The amount of N_2O in NH_3–NO/NO_2 SCR reactions ranks as NO_2 SCR > fast SCR > standard SCR at temperatures below 300°C. An interesting phenomenon was found, such that the maximum of N_2O formation was similar (98 ppm) at 300°C for both the fresh and aged MnNbCe catalysts in all the NH_3–NO/NO_2 SCR reactions.

It is a common sense that on V based catalysts, Fe/zeolite and Cu/Zeolite (Nova et al., 2006; Ciardelli et al., 2007; Grossale et al., 2008, 2009), N_2O formation increases as the NO_2 ratio increases in the feed, especially for NO_2 ratios over 50%. The maximum of N_2O formation occurs at 250–300°C in the NO_2 SCR reaction. N_2O formation is mainly ascribed to the decomposition of the NH_4NO_3 intermediate, which comes from NH_3 capturing the adsorbed nitrate species (Eq. (7)) (Grossale et al., 2008; Colombo et al., 2012; Shi et al., 2013).

$$NH_3 + HNO_3 \leftrightarrow NH_4NO_3 \rightarrow N_2O + 2H_2O \quad (7)$$

Meanwhile, Mn-base catalysts usually have the problem of low N_2 selectivity due to N_2O formation for standard SCR (Casapu et al., 2009; Tang et al., 2010; Zhang et al., 2011). In this study, the N_2O formation of the MnNbCe catalyst increased as the NO_2 ratio increased in the feed gas when the temperature was below 300°C. However, the N_2O formation over the MnNbCe catalyst was independent of NO_2 feed ratio at 300°C, being very similar at 95 ppm.

Hydrothermal aging leads to strong sintering and crystallization of Mn species and formation of $MnNb_2O_6$, accompanied by a decrease in the acidity and redox ability of the catalyst. The structural changes due to the hydrothermal

Table 2 – Amount of desorbed species over fresh NbMnCe catalysts.

Desorbed species	Without H_2O (ppm)	With H_2O (ppm)
NH_3	0.35	0.34
NO	0.14	0.29
NO_2 from NO + O_2 TPD	0.26	0.13
NO_2 from NO_2 TPD	0.96	0.96

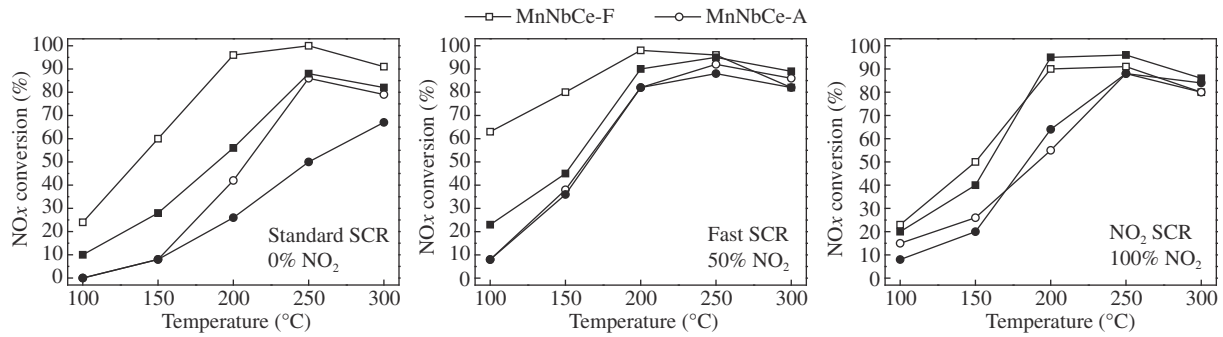

Fig. 6 – NH_3–NO/NO_2 SCR activities and the effects of water vapor over fresh and aged MnNbCe catalysts. (a) Standard SCR; (b) fast SCR; (c) NO_2 SCR. Reaction conditions: [NO] = [NH_3] = 500 ppm, [O_2] = 5%, [H_2O] = 10% if introduced, N_2 balances, GHSV 30,000 h^{-1}. Open symbol: without H_2O, filled symbol: with H_2O.

aging also decrease the catalytic activity of NH_3–NO/NO_2 SCR. An interesting point is that hydrothermal aging led to a decrease in the catalytic activity of NH_3–NO/NO_2 SCR, but N_2O formation for fresh and hydrothermally aged MnNbCe catalyst was similar. When water vapor was introduced into the feed gas, similar trends of N_2O formation were observed, with much less N_2O formed in the whole temperature range. Only around half as much N_2O was formed compared with that formed in the NH_3–NO/NO_2 SCR reaction without water vapor addition.

2.7. Influence of water vapor

The effect of water vapor on the NH_3-SCR reaction has been under an extensive study in the past decades, however the effect of water vapor on NH_3–NO/NO_2 SCR with various NO_2 ratios was still unclear. For the standard SCR reaction, previous studies (Qi and Yang, 2003a, b; Liu and He, 2010) confirmed that the effects of H_2O are mild and reversible when H_2O is removed, with only slight and reversible inhibition of NH_3/NO_x adsorption by H_2O. Magnusson et al. (2012) and co-workers reported that the addition of water vapor results in a decrease in NOx reduction and inhibition of N_2O formation. Bagnasco et al. (2000) reported that the addition of 1000 ppm H_2O results in a decrease in N_2O formation due to the inhibition of NH_3 oxidation, thus enhancing the reaction selectivity.

In this work, NH_3-TPD results indicated that water addition had a slight effect on the amount of NH_3 desorption. According to the literature (Liu and He, 2010), the presence of water vapor transformation of some Lewis acid sites into Brønsted acid sites is observed. Meanwhile, the effect of water vapor addition on NO + O_2TPD is much more severe, with the results showing only half as much NO_2 desorbed after water vapor addition. An interesting phenomenon is that water vapor addition barely affected pure NO_2 adsorption in NO_2 TPD. Therefore water vapor addition mainly affects the catalytic activity of the standard SCR reaction, with the influence weakening as the ratio of NO_2 increases, until no affect on the catalytic activity of NO_2 SCR is seen.

However, the formation of the byproduct N_2O is cut in half for all of the NH_3–NO/NO_2 SCR. As we discussed above, N_2O formation is mainly ascribed to the decomposition of the NH_4NO_3 intermediate. In the presence of enough water, the NH_4NO_3 tends to dissociate to NH_4^+ and NO_3^- ions, which decelerate its decomposition into N_2O and H_2O (Savara et al., 2008). As the catalytic activity of NO_2 SCR is similar in the absence and presence of water vapor, more NH_4NO_3 may directly decompose into N_2 and H_2O in the presence of water vapor.

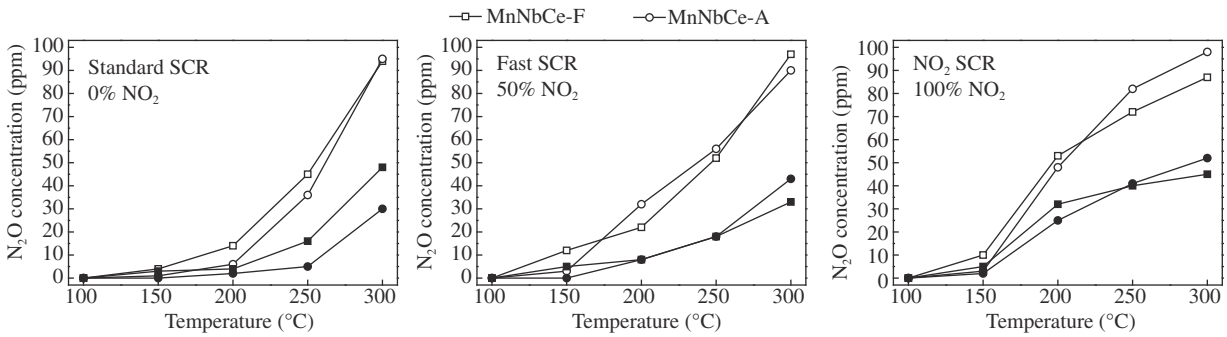

Fig. 7 – N_2O formation of NH_3–NO/NO_2 SCR over fresh and aged MnNbCe catalysts as a function of temperature. Reaction conditions: [NO] = [NH_3] = 500 ppm, [O_2] = 5%, N_2 balances, GHSV 30,000 h^{-1}. Open symbol: without H_2O, filled symbol: with H_2O.

3. Conclusions

The MnOx–NbOx–CeO_2 catalyst synthesized by the sol–gel method shows an excellent NH_3–NO/NO_2 SCR catalytic performance in the low temperature range of 150–300°C. Water vapor in the feed gas decreases the catalytic activity of standard SCR over the MnOx–NbOx–CeO_2 catalyst due to the inhibition of NOx adsorption. The influence was weakened when NO_2 was introduced in the feed gas, and water vapor addition barely affected the catalytic activity of NO_2 SCR. Meanwhile water vapor addition sharply decreased the N_2O formation by inhibiting the NH_4NO_3 decomposition into N_2O.

Acknowledgments

This work was supported by the Ministry of Science and Technology of China (No. 2010CB732304), the Science and Technology Department of Zhejiang Province Project (No. 2011C31010), and the National Natural Science Foundation of China (No. 51202126).

REFERENCES

Bagnasco, G., Busca, G., Galli, P., Massucci, M.A., Melanovád, K., Patronoe, P., et al., 2000. Selective reduction of NO with NH_3 on a new iron-vanadyl phosphate catalyst. Appl. Catal. B 28 (2), 135–142.

Carnö, J., Ferrandon, M., Björnbom, E., Järås, S., 1997. Mixed manganese oxide/platinum catalysts for total oxidation of model gas from wood boilers. Appl. Catal. A 155 (2), 265–281.

Casapu, M., Kröcher, O., Elsener, M., 2009. Screening of doped MnO_x–CeO_2 catalysts for low-temperature NO-SCR. Appl. Catal. B 88 (3–4), 413–419.

Casapu, M., Kröcher, O., Mehring, M., Nachtegaal, M., Borca, C., Harfouche, M., 2010. Characterization of Nb-containing MnO_x–CeO_2 catalyst for low-temperature selective catalytic reduction of NO with NH_3. J. Phys. Chem. C 114 (21), 9791–9801.

Casapu, M., Bernhard, A., Peitz, D., Mehring, M., Elsener, M., Kröcher, O., 2011. A niobia–ceria based multi-purpose catalyst for selective catalytic reduction of NO_x, urea hydrolysis and soot oxidation in diesel exhaust. Appl. Catal. B 103 (1–2), 79–84.

Chang, H.Z., Chen, X.Y., Li, J.H., Ma, L., Wang, C.Z., Liu, C.X., et al., 2013. Improvement of activity and SO_2 tolerance of Sn-modified MnO_x–CeO_2 catalysts for NH_3-SCR at low temperatures. Environ. Sci. Technol. 47 (10), 5294–5301.

Chen, L., Li, J.H., Ge, M.F., 2010. DRIFT study on cerium–tungsten/titiania catalyst for selective catalytic reduction of NO_x with NH_3. Environ. Sci. Technol. 44 (24), 9590–9596.

Ciardelli, C., Nova, I., Tronconi, E., Chatterjee, D., Bandl-Konrad, B., Weibel, M., et al., 2007. Reactivity of NO/NO_2–NH_3 SCR system for diesel exhaust aftertreatment: identification of the reaction network as a function of temperature and NO_2 feed content. Appl. Catal. B 70 (1–4), 80–90.

Colombo, M., Nova, I., Tronconi, E., Schmeißer, V., Bandl-Konrad, B., Zimmermann, L., 2012. NO/NO_2/N_2O–NH_3 SCR reactions over a commercial Fe-zeolite catalyst for diesel exhaust aftertreatment: intrinsic kinetics and monolith converter modelling. Appl. Catal. B 111–112, 106–118.

Du, X.S., Gao, X., Fu, Y.C., Gao, F., Luo, Z.Y., Cen, K.F., 2012. The co-effect of Sb and Nb on the SCR performance of the V_2O_5/TiO_2 catalyst. J. Colloid Interface Sci. 368 (1), 406–412.

Ettireddy, P.R., Ettireddy, N., Mamedov, S., Boolchand, P., Smirniotis, P.G., 2007. Surface characterization studies of TiO_2 supported manganese oxide catalysts for low temperature SCR of NO with NH_3. Appl. Catal. B 76 (1–2), 123–134.

Grossale, A., Nova, I., Tronconi, E., Chatterjee, D., Weibel, M., 2008. The chemistry of the NO/NO_2–NH_3 "fast" SCR reaction over Fe-ZSM5 investigated by transient reaction analysis. J. Catal. 256 (2), 312–322.

Grossale, A., Nova, I., Tronconi, E., Chatterjee, D., Weibel, M., 2009. NH_3–NO/NO_2 SCR for diesel exhausts aftertreatment: Reactivity, mechanism and kinetic modelling of commercial Fe- and Cu-promoted zeolite catalysts. Top. Catal. 52 (13–20), 1837–1841.

Iwasaki, M., Shinjoh, H., 2010. A comparative study of "standard", "fast" and "NO_2" SCR reactions over Fe/zeolite catalyst. Appl. Catal. A 390 (1–2), 71–77.

Jin, R.B., Liu, Y., Wu, Z.B., Wang, H.Q., Gu, T.T., 2010. Low-temperature selective catalytic reduction of NO with NH_3 over Mn–Ce oxides supported on TiO_2 and Al_2O_3: a comparative study. Chemosphere 78 (9), 1160–1166.

Kato, A., Matsuda, S., Kamo, T., Nakajima, F., Kuroda, H., Narita, T., 1981. Reaction between NO_x and NH_3 on iron oxide–titanium oxide catalyst. J. Phys. Chem. 85 (26), 4099–4102.

Kim, S.S., Choi, S.H., Hong, S.C., 2010. Redox characteristics of O_2 and NO_2 in the fast NH_3-selective catalytic reduction of NO_x over vanadium-based catalyst. Environ. Eng. Sci. 27 (10), 845–852.

Koebel, M., Madia, G., Elsener, M., 2002. Selective catalytic reduction of NO and NO_2 at low temperatures. Catal. Today 73 (3–4), 239–247.

Larrubia, M.A., Ramis, G., Busca, G., 2000. An FT-IR study of the adsorption of urea and ammonia over V_2O_5–MoO_3–TiO_2 SCR catalysts. Appl. Catal. B 27 (3), L145–L151.

Larrubia, M.A., Ramis, G., Busca, G., 2001. An FT-IR study of the adsorption and oxidation of N-containing compounds over Fe_2O_3–TiO_2 SCR catalysts. Appl. Catal. B 30 (1–2), 101–110.

Li, H.F., Lu, G.Z., Dai, Q.G., Wang, Y.Q., Guo, Y., Guo, Y.L., 2011a. Efficient low-temperature catalytic combustion of trichloroethylene over flower-like mesoporous Mn-doped CeO_2 microspheres. Appl. Catal. B 102 (3–4), 475–483.

Li, J.H., Chang, H.Z., Ma, L., Hao, J.M., Yang, R.T., 2011b. Low-temperature selective catalytic reduction of NO_x with NH_3 over metal oxide and zeolite catalysts—a review. Catal. Today 175 (1), 147–156.

Liu, F.D., He, H., 2010. Selective catalytic reduction of NO with NH_3 over manganese substituted iron titanate catalyst: reaction mechanism and H_2O/SO_2 inhibition mechanism study. Catal. Today 153 (3–4), 70–76.

Liu, Z.M., Zhang, S.X., Li, J.H., Ma, L.L., 2014. Promoting effect of MoO_3 on the NO_x reduction by NH_3 over CeO_2/TiO_2 catalyst studied with *in situ* DRIFTS. Appl. Catal. B 144, 90–95.

Ma, Z.R., Weng, D., Wu, X.D., Si, Z.C., Wang, B., 2012. A novel Nb–Ce/WOx–TiO_2 catalyst with high NH_3-SCR activity and stability. Catal. Commun. 27, 97–100.

Magnusson, M., Fridell, E., Ingelsten, H.H., 2012. The influence of sulfur dioxide and water on the performance of a marine SCR catalyst. Appl. Catal. B 111–112, 20–26.

Nova, I., Ciardelli, C., Tronconi, E., Chatterjee, D., Bandl-Konrad, B., 2006. NH_3–NO/NO_2 chemistry over V-based catalysts and its role in the mechanism of the fast SCR reaction. Catal. Today 114 (1), 3–12.

Qi, G.S., Yang, R.T., 2003a. Performance and kinetics study for low-temperature SCR of NO with NH_3 over MnO_x–CeO_2 catalyst. J. Catal. 217 (2), 434–441.

Qi, G.S., Yang, R.T., 2003b. Low-temperature selective catalytic reduction of NO with NH_3 over iron and manganese oxides supported on titania. Appl. Catal. B 44 (3), 217–225.

Qi, G.S., Yang, R.T., 2004. Characterization and FTIR studies of MnO_x–CeO_2 catalyst for low-temperature selective catalytic reduction of NO with NH_3. J. Phys. Chem. B 108 (40), 15738–15747.

Qi, G.S., Yang, R.T., Chang, R., 2004. MnO_x–CeO_2 mixed oxides prepared by co-precipitation for selective catalytic reduction of NO with NH_3 at low temperatures. Appl. Catal. B 51 (2), 93–106.

Qu, R.Y., Gao, X., Cen, K.F., Li, J.H., 2014. Relationship between structure and performance of a novel cerium–niobium binary oxide catalyst for selective catalytic reduction of NO with NH_3. Appl. Catal. B 142–143, 290–297.

Ramis, G., Yi, L., Busca, G., Turco, M., Kotur, E., Willey, R.J., 1995. Adsorption, activation, and oxidation of ammonia over SCR catalysts. J. Catal. 157 (2), 523–535.

Ruggeri, M.P., Grossale, A., Nova, I., Tronconi, E., Jirglova, H., Sobalik, Z., 2012. FTIR *in situ* mechanistic study of the NH_3–NO/NO_2 "Fast SCR" reaction over a commercial Fe-ZSM-5 catalyst. Catal. Today 184 (1), 107–114.

Savara, A., Li, M.J., Sachtler, W.M.H., Weitz, E., 2008. Catalytic reduction of NH_4NO_3 by NO: effects of solid acids and implications for low temperature DeNOx processes. Appl. Catal. B 81 (3–4), 251–257.

Shen, B.X., Liu, T., Zhao, N., Yang, X.Y., Deng, L.D., 2010. Iron-doped Mn–Ce/TiO_2 catalyst for low temperature selective catalytic reduction of NO with NH_3. J. Environ. Sci. 22 (9), 1447–1454.

Shen, B.X., Liu, T., Yang, X.Y., Zhao, N., 2011. MnO_x/$Ce_{0.6}Zr_{0.4}O_2$ catalysts for low-temperature selective catalytic reduction of NO_x with NH_3. Environ. Eng. Sci. 28 (4), 291–298.

Shen, B.X., Zhang, X.P., Ma, H.Q., Yao, Y., Liu, T., 2013. A comparative study of Mn/CeO_2, Mn/ZrO_2 and Mn/Ce–ZrO_2 for low temperature selective catalytic reduction of NO with NH_3 in the presence of SO_2 and H_2O. J. Environ. Sci. 25 (4), 791–800.

Shen, B.X., Ma, H.Q., He, C., Zhang, X.P., 2014. Low temperature NH_3-SCR over Zr and Ce pillared clay based catalysts. Fuel Process. Technol. 119, 121–129.

Shi, X.Y., Liu, F.D., Xie, L.J., Shan, W.P., He, H., 2013. NH_3-SCR performance of fresh and hydrothermally aged Fe-ZSM-5 in standard and fast selective catalytic reduction reactions. Environ. Sci. Technol. 47 (7), 3293–3298.

Sun, D.K., Liu, Q.Y., Liu, Z.Y., Gui, G.Q., Huang, Z.G., 2009. Adsorption and oxidation of NH_3 over V_2O_5/AC surface. Appl. Catal. B 92 (3–4), 462–467.

Tang, X.F., Li, Y.G., Huang, X.M., Xu, Y.D., Zhu, H.Q., Wang, J.G., et al., 2006. MnO_x–CeO_2 mixed oxide catalysts for complete oxidation of formaldehyde: effect of preparation method and calcination temperature. Appl. Catal. B 62 (3–4), 265–273.

Tang, X.F., Li, J.H., Sun, L., Hao, J.M., 2010. Origination of N_2O from NO reduction by NH_3 over β-MnO_2 and α-Mn_2O_3. Appl. Catal. B 99 (1–2), 156–162.

Tronconi, E., Nova, I., Ciardelli, C., Chatterjee, D., Weibel, M., 2007. Redox features in the catalytic mechanism of the "standard" and "fast" NH_3-SCR of NOx over a V-based catalyst investigated by dynamic methods. J. Catal. 245 (1), 1–10.

Xu, H.D., Zhang, Q.L., Qiu, C.T., Lin, T., Gong, M.C., Chen, Y.Q., 2012. Tungsten modified MnO_x–CeO_2/ZrO_2 monolith catalysts for selective catalytic reduction of NO_x with ammonia. Chem. Eng. Sci. 76, 120–128.

Zawadzki, J., Wiśniewski, M., 2003. *In situ* characterization of interaction of ammonia with carbon surface in oxygen atmosphere. Carbon 41 (12), 2257–2267.

Zhang, Q.L., Qiu, C.T., Xu, H.D., Lin, T., Gong, M.C., Chen, Y.Q., 2011. Novel promoting effects of tungsten on the selective catalytic reduction of NO by NH_3 over MnO_x–CeO_2 monolith catalyst. Catal. Commun. 16 (1), 20–24.

Editorial Board of Journal of Environmental Sciences

JOURNAL OF ENVIRONMENTAL SCIENCES

环境科学学报(英文版)

www.jesc.ac.cn

Aims and scope

Journal of Environmental Sciences is an international academic journal supervised by Research Center for Eco-Environmental Sciences, Chinese Academy of Sciences. The journal publishes original, peer-reviewed innovative research and valuable findings in environmental sciences. The types of articles published are research article, critical review, rapid communications, and special issues.

The scope of the journal embraces the treatment processes for natural groundwater, municipal, agricultural and industrial water and wastewaters; physical and chemical methods for limitation of pollutants emission into the atmospheric environment; chemical and biological and phytoremediation of contaminated soil; fate and transport of pollutants in environments; toxicological effects of terrorist chemical release on the natural environment and human health; development of environmental catalysts and materials.

For subscription to electronic edition

Elsevier is responsible for subscription of the journal. Please subscribe to the journal via http://www.elsevier.com/locate/jes.

For subscription to print edition

China: Please contact the customer service, Science Press, 16 Donghuangchenggen North Street, Beijing 100717, China. Tel: +86-10-64017032; E-mail: journal@mail.sciencep.com, or the local post office throughout China (domestic postcode: 2-580).

Outside China: Please order the journal from the Elsevier Customer Service Department at the Regional Sales Office nearest you.

Submission declaration

Submission of the work described has not been published previously (except in the form of an abstract or as part of a published lecture or academic thesis), that it is not under consideration for publication elsewhere. The publication should be approved by all authors and tacitly or explicitly by the responsible authorities where the work was carried out. If the manuscript accepted, it will not be published elsewhere in the same form, in English or in any other language, including electronically without the written consent of the copyright-holder.

Editorial

Authors should submit manuscript online at http://www.jesc.ac.cn. In case of queries, please contact editorial office, Tel: +86-10-62920553, E-mail: jesc@rcees.ac.cn. Instruction to authors is available at http://www.jesc.ac.cn.

Journal of Environmental Sciences (Established in 1989)
Volume 31 2015

Supervised by	Chinese Academy of Sciences	**Published by**	Science Press, Beijing, China
Sponsored by	Research Center for Eco-Environmental		Elsevier Limited, The Netherlands
	Sciences, Chinese Academy of Sciences	**Distributed by**	
Edited by	Editorial Office of Journal of	Domestic	Science Press, 16 Donghuangchenggen
	Environmental Sciences		North Street, Beijing 100717, China
	P. O. Box 2871, Beijing 100085, China		Local Post Offices through China
	Tel: 86-10-62920553; http://www.jesc.ac.cn	Foreign	Elsevier Limited
	E-mail: jesc@rcees.ac.cn		http://www.elsevier.com/locate/jes
Editor-in-chief	X. Chris Le	**Printed by**	Beijing Beilin Printing House, 100083, China

CN 11-2629/X **Domestic postcode: 2-580** **Domestic price per issue RMB ¥ 110.00**

ISSN 1001-0742